THE JOURNAL OF PHYSICAL CHEMISTRY B

ARTICLE

pubs.acs.org/JPCB

An FCS Study of Unfolding and Refolding of CPM-Labeled Human Serum Albumin: Role of Ionic Liquid

Dibyendu Kumar Sasmal,[†] Tridib Mondal,[†] Supratik Sen Mojumdar,[†] Aparajita Choudhury,[‡] Rajat Banerjee,[‡] and Kankan Bhattacharyya*[,†]

[†]Department of Physical Chemistry, Indian Association for the Cultivation of Science, Jadavpur, Kolkata 700032, India

[‡]Dr. B. C. Guha Centre for Genetic Engineering and Biotechnology and Department of Biotechnology, University of Calcutta, Ballygunge Circular Road, Kolkata 700019, India

ABSTRACT: The effect of a room temperature ionic liquid (RTIL) on the conformational dynamics of a protein, human serum albumin (HSA), is studied by fluorescence correlation spectroscopy (FCS). For this, the protein was covalently labeled by a fluorophore, 7-dimethylamino-3-(4-maleimidophenyl)-4-methylcoumarin (CPM). On addition of a RTIL ([pmim][Br]) to the native protein, the diffusion coefficient (D_t) decreases and the hydrodynamic radius (R_h) increases. This suggests that the RTIL ([pmim][Br]) acts as a denaturant when the protein is in the native state. However, addition of [pmim][Br] to a protein denatured by GdnHCl causes an increases in D_t and decrease in R_h. This suggests that in the presence of GdnHCl addition of RTIL helps the protein to refold. In the native state, the conformational dynamics of protein is described by three distinct time constants: ~3.6 ± 0.7, ~29 ± 4.5, and 133 ± 23 μs. The faster components (~3.6 ± 0.7 and ~29 ± 4.5 μs) are ascribed to chain dynamics of the protein, while the slowest component (133 μs) is responsible for interchain interaction or concerted motion. On addition of [pmim][Br], the conformational dynamics of HSA becomes slower (~5.1 ± 1, ~43.5 ± 2.8, and ~311 ± 2.3 μs in the presence of 1.5 M [pmim][Br]). The time constants for the protein denatured by 6 M GdnHCl are 3.2 ± 0.4, 34 ± 6, and 207 ± 38 μs. When 1.5 M [pmim][Br] is added to the denatured protein (in 6 M GdnHCl), the time constants become ~5 ± 1, ~41 ± 10, and ~230 ± 45 μs. The lifetime histogram shows that, on addition of GdnHCl to HSA, the contribution of the shorter lifetime component decreases and vanishes at 6 M GdnHCl. The shorter lifetime component immediately reappears after addition of RTIL to unfolded HSA. This suggests recoiling of the unfolded protein by RTIL.

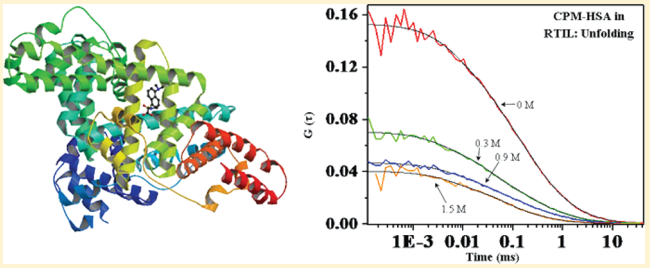

1. INTRODUCTION

Fluorescence correlation spectroscopy (FCS) is an elegant and sensitive technique for studying diffusion as well as dynamics in submicrosecond-to-second time scales.[1−6] The fluctuations of fluorescence observed in FCS may result either from a change in the number of fluorophores in the observation volume due to diffusion, a change in fluorescence properties of the molecule as a consequence of a chemical reaction (e.g., quenching), or a conformational fluctuation.[1,2] Conformational fluctuations associated with folding pathways for protein,[1,2] RNA,[3] and DNA[4a] have been studied by many groups by FCS. Webb and co-workers[1b,c] studied the structural fluctuation of acid-denatured apomyoglobin (apoMb) by FCS. They showed that as the pH decreases from 6.3 (native state) to 4.1 (molten globule) the contribution of the 100 μs component increases from 3 to 10% while that of the 8 μs component increases from 7 to 12%. At still lower pH (<4.1), a 200 μs component is observed whose contribution remains constant at 10%. The 200 μs component is close to the protein diffusion time for apoMb.[1b,c] From pH 4.1 to pH 2.6 (unfolded), the amplitude of a 30 μs component increases from 11 to 17%. Lu and co-workers carefully analyzed the in-homogeneity of conformational dynamics in proteins and its implication in enzyme kinetics and cell signaling using single molecule photon stamping measurement.[2] Neuweiler et al. studied single-molecule fluorescence quenching by photoinduced electron transfer (PET-FCS) to investigate the folding dynamics of the small binding domain BBL.[4b] Chattopadhayay et al. detected a relaxation time of 35 μs for the protein, IFABP (15 kDa),[6a] and determined the exact size of the unfolding intermediates.[6b] Haran and co-workers discussed how the diffusion coefficient (D_t) of a protein (adenylate kinase, AK) may be determined accurately even in the presence of a high concentration of cosolutes that changes the refractive index and viscosity significantly.[7]

The main aim of the present study is to understand how a room temperature ionic liquid (RTIL) affect protein dynamics. In recent years, room temperature ionic liquids (RTILs) have found applications in biology ranging from bioanalysis to cellulose processing[8] and also for biosensors and biocatalysis.[8,9] The structure of a protein in a neat RTIL depends on hydrogen

Received: August 15, 2011
Revised: September 20, 2011
Published: September 27, 2011

Scheme 1. (A) Structure of Human Serum Albumin (HSA) Covalently Labeled with CPM at cys-34 (from Protein Data Bank ID: 2XVQ); (B) [pmim][Br]; (C) CPM

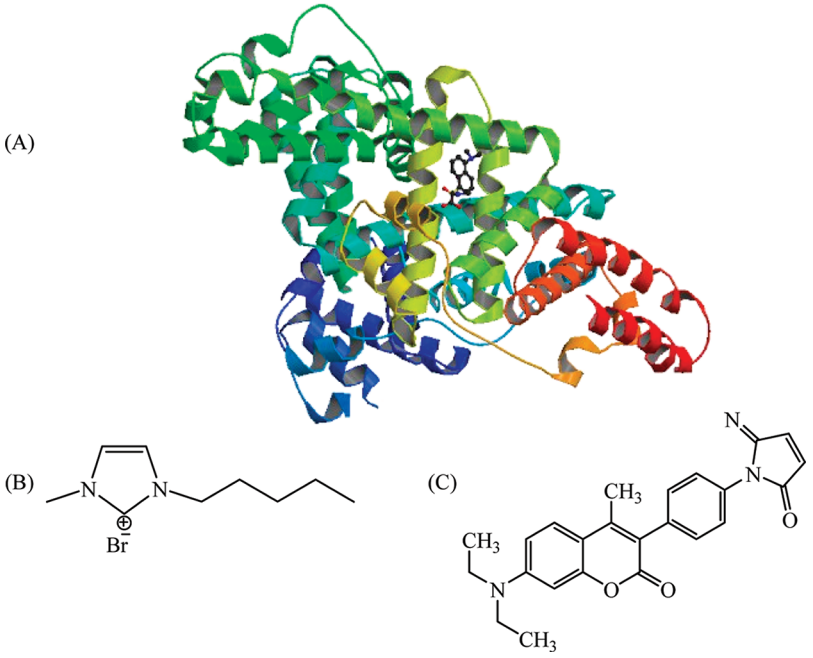

bonding, polarity (hydrophobicity, dielectric constant), nanostructure, and solvent viscosity.[10] Strong coordination of a RTIL ion to protein can be an important factor favoring dissolution, but the same may disrupt the intermolecular interactions responsible for native structure. For example, mixtures of the salt choline dihydrogen phosphate with water not only dissolve cytochrome *c* (cyt *c*), but, kept at room temperature, sustain notable enzyme activity for over a year.[11] In one of the first thermodynamic studies of the stability of protein in RTIL, Baker and co-workers showed significant stabilization of proteins at elevated temperatures by RTIL in comparison to water.[12] To understand the effect of the ions of a RTIL, the Hofmeister series may be useful as a guide for ion-specific protein stability and activity in the native state.[10b] There are several experimental studies[13] and molecular dynamics simulations[14] to predict the structure and stability of different proteins in RTIL. Bright and his co-workers studied the behavior of HSA protein labeled with acrylodan at cys-34.[13g] They found that the structure and function of the protein depends on both the nature of the protein and RTIL and its level of hydration.[13g] Flower II and his co-workers showed that a RTIL (ethylammonium nitrate, EAN) may be used to enhance the recovery of denatured hen egg lysozyme.[15] They reported that when lysozyme was denatured using routine procedures and is renatured using EAN as an additive, it regains 75% of its activity. When the protein was denatured and reduced in neat EAN, dilution resulted in over 90% recovery of active protein.[15a] Atkins and his co-workers showed that a RTIL (propyammonium formate, PAF) denatures protein spontaneously because of binding of the PA^+ ion of the RTIL to the hydrophobic core of the protein.[13c] Constatinescu et al. showed that RTILs can promote the stability of the native state, accelerate refolding, and suppress irreversible aggregation.[10b] They may also affect the self-assembly of small oligomers to larger aggregates, precipitates, and amyloid fibrils.[10b] Further, they showed that choline dihydrogenphosphate ([col][dhp]) enhances the thermal stability of ribonuclease A, whereas 1-ethyl-3-methylimidozolium dicynamide ([emim][dca]) may act as a strong denaturant.[10b]

While the effect of RTIL on protein has been studied by many techniques, single molecule spectroscopy (SMS) has not been applied so far to study the effect of a RTIL on the conformational dynamics and folding of a protein labeled with a covalent probe. In this work, we report the study of conformational dynamics of protein using fluorescence correlation spectroscopy (FCS). For this, we have covalently labeled a protein (HSA) by a fluorophore 7-dimethylamino-3-(4-maleimidophenyl)-4-methylcoumarin (CPM). HSA has been reported to have five principle binding sites for a long or medium chain fatty acid, three of which bind quite strongly.[16,17] The binding sites in HSA may be classified as hydrophobic and hydrophilic domains.[16] Sudlow and co-workers showed that the principal ligand binding sites are located in subdomains IIA and IIIA.[17b,c] Of these, site IIA binds hydrophilic (polar or charged) ligands and IIIA binds hydrophobic groups. The lone tryptophan residue of HSA has been shown to be a part of site IIA because modification of tryptophan reduces warfarin binding.[17b] The lone free cysteine (cys-34) is located in domain I.[17]

We have previously reported that if a solvation probe (CPM) is covalently attached to the free SH group (cysteine-34 of HSA) it resides close to a surfactant binding site and report the effect of SDS binding to HSA.[18] We now investigate the effect of RTIL on the size and dynamics of both the native and unfolded state (denatured by GdnHCl) of HSA protein.

2. EXPERIMENTAL SECTION

2.1. Protein Labeling and Sample Preparation for FCS Experiment. Laser-grade CPM (7-dimethylamino-3-(4-maleimidophenyl)-4-methylcoumarin, Exciton) was used as received.

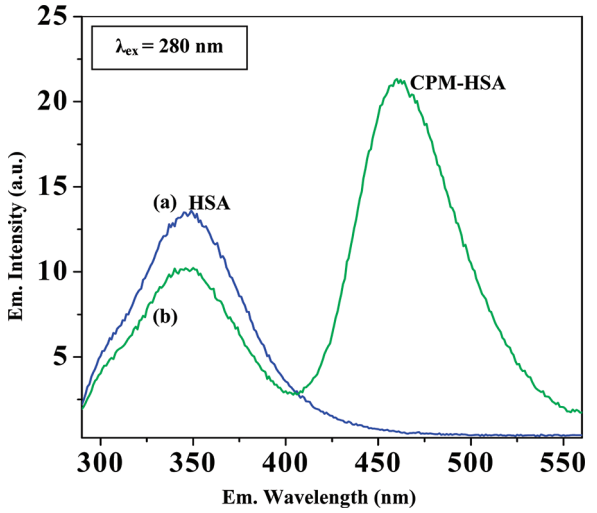

Figure 1. (a) Tryptophan emission (λ_{ex} = 280 nm) of HSA in phosphate buffer solution (pH 7.0). (b) Tryptophan emission of HSA when CPM is covalently attached with the free thiol group (−SH) of the cysteine-34 position of HSA molecule in phosphate buffer (pH 7.0). The quenching of tryptophan emission is due to the fluorescence resonance energy transfer (FRET) from it to the CPM molecule attached to the same protein. The emission peak at 460 nm is for CPM attached to HSA.

Human serum albumin (HSA) was purchased from Sigma and used without further purification. The steady-state absorption and emission spectra were recorded with a Shimadzu UV-2401 spectrophotometer and a Spex FluoroMax-3 spectro-fluorimeter, respectively.

The covalent labeling of HSA binding of CPM at the free cys-34 residue (Micheal addition reaction, Scheme 1) was carried out following the method reported by Wang et al.,[19] with minor modifications.[18] A stock solution of HSA (70 μM) was prepared in 0.1 M phosphate buffer (pH 7.0). A sufficient quantity of CPM (in minimum amount of *N*,*N*-dimethyl formamide) was added to 10 mL of this solution to yield a molar ratio of HSA to CPM of 1:1. The mixture was stirred gently and maintained at room temperature for 10 h. It was then dialyzed for 2 days at 4 °C against 500 mL of phosphate buffer (0.1 M) with a change of dialysis buffer after every 6 h. The labeled protein was then passed through a Sephadex G-50 gel column for further removal of any unreacted and free CPM and HSA. The concentration of labeled protein was measured by the method of Lowry et al.[19b] The concentration of CPM labeled to the protein, HSA, was determined to be ~22 μM by optical absorbance.

The synthesis of the ionic liquid, [pmim][Br], is described in our previous publications.[20] For steady-state FRET studies (lone tryptophan of HSA to CPM at cys-34), we used the same undiluted solution obtained after dialysis and running through the Sephadex gel. However, for the FCS experiment, we diluted the solution such that the CPM concentration is about 1 nM. In the FCS experiment, Tween-20 (0.005%) was used as a solvent additive to suppress attachment of the protein to the glass surface. The pH of the solution was kept at 7.0, and all the FCS experiments were carried out at 20 °C.

2.2. FCS Measurements. FCS studies of the protein samples (~1 nM CPM) were carried out in a confocal setup (PicoQuant, MicroTime 200) with an inverted optical microscope (Olympus IX-71). A water immersion objective (60×1.2 NA) was used to

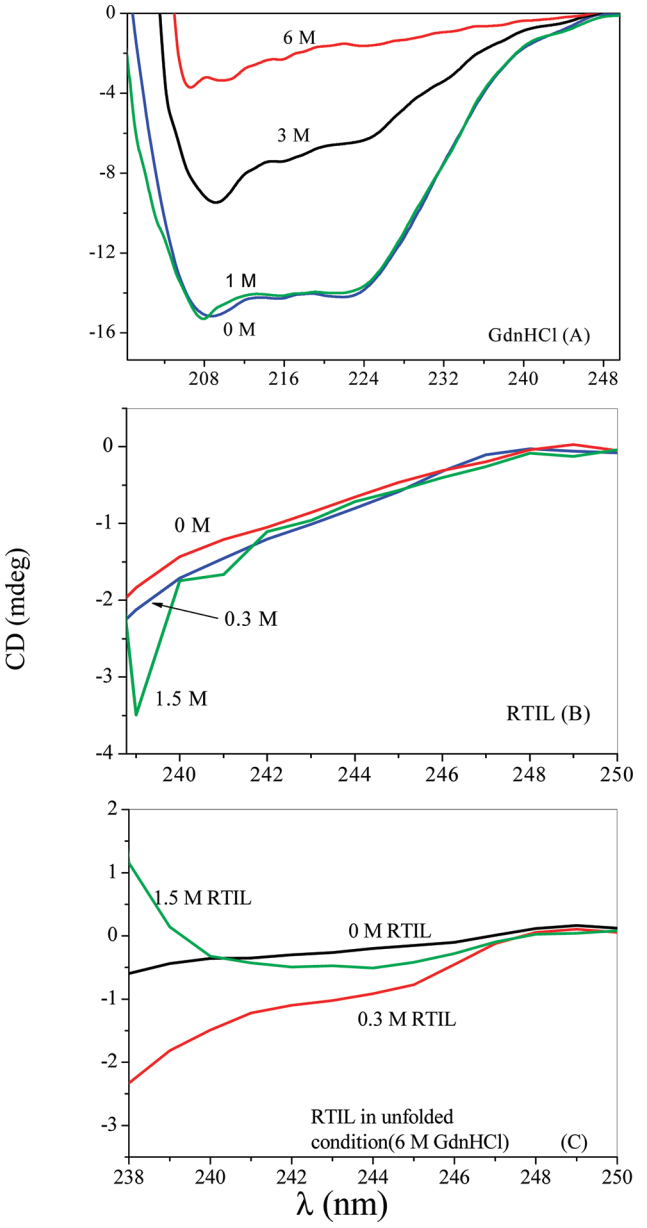

Figure 2. CD spectra of HSA, at different concentrations of (A) GdnHCl, (B) RTIL, and (C) RTIL under fully denatured conditions (6 M GdnHCl). RTIL itself absorbs significantly below 235 nm. Thus, the CD spectra could not be recorded below 235 nm in the presence of RTIL.

focus the excitation light (405 nm) from a pulsed diode laser (PDL 828-S "SEPIA II", PicoQuant) onto the sample placed on a coverslip (~50 μL). The fluorophore was excited at λ_{ex} = 405 nm using a picosecond diode with stable repetition rate (20 MHz). To separate the fluorescence from the exciting laser (along the same path), we used a dichroic mirror and appropriate band-pass filters (HQ430lp, Chroma). To collect the fluorescence, a suitable band-pass filter (HQ480/40, Chroma) was used. The fluorescence was then focused through a pinhole (50 μm) onto a 50/50 beam splitter (Chroma) prior to entering two single-photon counting avalanche photodiodes (SPADs). The fluorescence autocorrelation traces were recorded by using two detectors (SPAD1

and SPAD2). Through the use of two detectors, the artifacts arising from the after pulse are eliminated. The signal was subsequently processed by the PicoHarp-300 time-correlated single photon counting card (PicoQuant) to generate the autocorrelation function, $G(\tau)$. The data was collected in time-tagged time-resolved (TTTR) mode.

The autocorrelation function is very sensitive to the collar settings of the microscope objective.[6b] We fixed the objective collar setting to 0.17 for each experiment.

2.3. FCS Data Modeling and Analysis. In FCS, the autocorrelation function $G(\tau)$ of fluorescence intensity $I(t)$ is defined as

$$G(\tau) = \frac{\langle I(t)I(t+\tau)\rangle}{\langle I(t)\rangle\langle I(t+\tau)\rangle} \quad (1)$$

where $G(\tau)$ is calculated for all accessible time lags τ and $\langle I(t)\rangle = \langle I(t+\tau)\rangle$ for stationary processes. In case of free diffusion of a two-state fluorophore diffusing in a 3D Gaussian excitation volume of widths ω_{xy} and ω_z

$$G_D(\tau) = \frac{1}{N}\left[1 + \frac{\tau}{\tau_D}\right]^{-1}\left[1 + \frac{\tau}{\omega^2\tau_D}\right]^{-1/2} \quad (2)$$

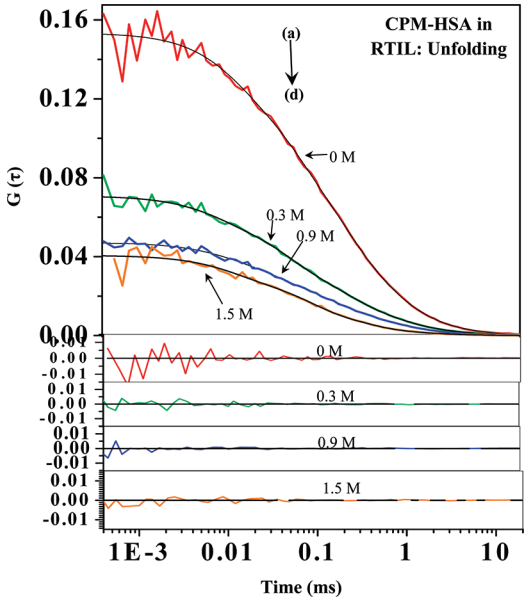

Figure 3. The autocorrelation traces with their best fit line of CPM labeled HSA (a) under native conditions and after addition of (b) 0.3 M [pmim][Br], (c) 0.9 M [pmim][Br], and (d) 1.5 M [pmim][Br] solution to the native HSA. From the amplitude of the curves, $G(\tau)$, it would appear the number of molecules (N) in the beam increases with the increase of RTIL concentration. Residuals are shown in the lower part of the figure with the corresponding color of the curves.

where N is the number of molecules in the observed volume, τ_D is the diffusion time of species

$$\tau_D = \frac{\omega_{xy}^2}{4D} \quad (3)$$

and $\omega = \omega_z/\omega_{xy}$ which is the height-to-diameter ratio of the 3D Gaussian confocal volume. The structure parameter (ω) of the excitation volume was calibrated using a sample (R6G in water) of known diffusion coefficient (D_t = 426 μm^2 s^{-1}).[21a] The estimated volume of the excitation volume is ~0.75 fL with a transverse radius (ω_{xy}) ~ 305 nm. If the sample is undergoing conformational fluctuation among the multiple states, then they can be distinguished by their fluorescence quantum yield. We assume that there is no detectable change in τ_D among the states. Then, the correlation function is

$$G(t) = G_D(\tau)G_F(\tau) \quad (4)$$

where $G_F(\tau)$ is the contribution from fluctuation to the correlation function.

We analyzed all the raw FCS data by the fitting software IgorPro 6. The correlation function data for all the systems can be fitted successfully by using the following equation:[1b]

$$G_D(\tau) = \frac{1}{N}\left[1 + \frac{\tau}{\tau_D}\right]^{-1}\left[1 + \frac{\tau}{\omega^2\tau_D}\right]^{-1/2}\left[1 + A_1e^{-\tau/\tau_{R_1}} + A_2e^{-\tau/\tau_{R_2}} + A_3e^{-\tau/\tau_{R_3}}\right] \quad (5)$$

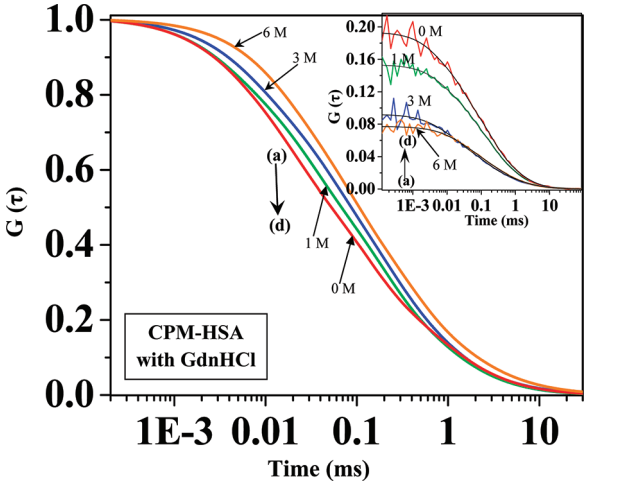

Figure 4. The normalized best fit line of the autocorrelation curves of CPM labeled HSA on addition of (a) 6 M GdnHCl, (b) 3 M GdnHCl, (c) 1 M GdnHCl, and (d) buffer. The inset shows the autocorrelation curves with their best fit line. From the amplitude of the curves, $G(\tau)$, in the inset, it would appear the number of molecules (N) in the beam increases with the increase of GdnHCl concentration.

Table 1. Effect of a RTIL ([pmim][Br]) on the Diffusion (ms) and Relaxation (μs) Time of Native Human Serum Albumin (HSA) Labeled with CPM

[pmim][Br]	τ_D (ms)	τ_{R1} (μs) (A_1)	τ_{R2} (μs) (A_2)	τ_{R3} (μs) (A_3)	D_t (μm^2/s)	R_h (Å)
0 M	0.40 ± 0.02	3.6 ± 0.7 (0.28)	29 ± 4.5 (0.39)	133 ± 23 (0.33)	56.3 ± 2.7	38.4 ± 2.0
0.3 M	0.73 ± 0.03	3.2 ± 0.6 (0.24)	29 ± 3.5 (0.42)	230 ± 45 (0.35)	30.8 ± 1.2	53.5 ± 2.0
0.9 M	0.92 ± 0.05	5.4 ± 0.9 (0.24)	41 ± 6.5 (0.44)	325 ± 60 (0.31)	24.5 ± 1.3	59.4 ± 3.0
1.5 M	1.20 ± 0.04	5.1 ± 1 (0.20)	43.5 ± 2.8 (0.45)	311 ± 50 (0.37)	18.8 ± 0.7	60.9 ± 2.0

dx.doi.org/10.1021/jp207829y |J. Phys. Chem. B 2011, 115, 13075–13083

Table 2. Diffusion (ms) and Relaxation (μs) Times of Human Serum Albumin (HSA) Labeled CPM with Different Concentrations of Denaturant GdnHCl

[GdnHCl]	τ_D (ms)	τ_{R1} (μs) (A_1)	τ_{R2} (μs) (A_2)	τ_{R3} (μs) (A_3)	D_t ($\mu m^2/s$)	R_h (Å)
0 M	0.40 ± 0.02	3.6 ± 0.7 (0.28)	29 ± 4.5 (0.39)	133 ± 23 (0.33)	56.3 ± 2.7	38.4 ± 2.0
1 M	0.42 ± 0.02	3.5 ± 0.5 (0.22)	22 ± 5 (0.39)	124 ± 20 (0.39)	53.6 ± 2.5	38.3 ± 1.8
2 M	0.48 ± 0.03	3.3 ± 0.6 (0.29)	23 ± 3.5 (0.33)	135 ± 26 (0.38)	46.9 ± 2.8	43.1 ± 2.6
3 M	0.53 ± 0.02	3.8 ± 0.9 (0.28)	31 ± 6 (0.42)	184 ± 30 (0.30)	42.5 ± 1.6	46.3 ± 1.7
4 M	0.66 ± 0.03	3.2 ± 0.7 (0.21)	31 ± 4.5 (0.46)	205 ± 32 (0.33)	34.1 ± 1.5	56.6 ± 2.5
5 M	0.71 ± 0.03	3.6 ± 0.5 (0.27)	31 ± 5 (0.39)	204 ± 35 (0.34)	31.7 ± 1.3	58.2 ± 2.5
6 M	0.765 ± 0.04	3.2 ± 0.4 (0.16)	34 ± 6 (0.43)	207 ± 38 (0.41)	29.4 ± 1.5	61.0 ± 3.0

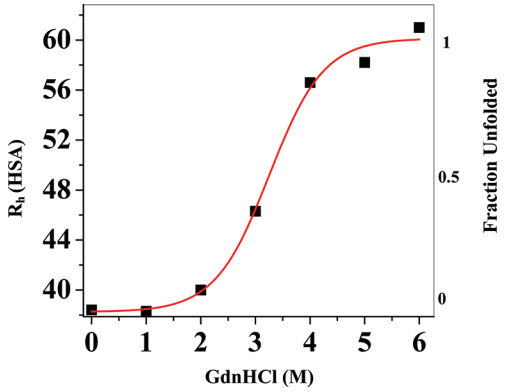

Figure 5. Hydrodynamic radii (R_h) of protein HSA (black squares), plotted with the concentration (in M) of denaturant, GdnHCl.

where τ_R is the relaxation time for an exponential component with an associated amplitude A. We call it the 3-component-3D diffusion model.

According to the Stokes−Einstein equation, R_h can be determined from the measured value of D_t of the diffusing species as follows

$$D_t = \frac{k_B T}{6\pi\eta R_h} \tag{6}$$

where η is the viscosity of the solution and R_h is the hydrodynamic radius.

Addition of RTIL affects the viscosity and refractive index, and this may affect determination of the size of the proteins (R_h). We have correctly determined R_h taking into account the refractive index mismatch and viscosity correction as discussed by Chattopadhyay[6] and Sherman et al.[7]

Sherman et al.[7] used R6G as a diffusion standard and used the ratio method to eliminate the errors due to refractive index mismatch and viscosity. We avoided R6G as a diffusion standard because R6G is positively charged and may interact with the ions of RTIL and GdnHCl. Instead, we used C480 as a diffusion standard and used the following equation:

$$\frac{R_h^{\text{Protein}}}{R_h^{\text{C480}}} = \frac{\tau_D^{\text{Protein}}}{\tau_D^{\text{C480}}} \tag{7}$$

Since C480 is a rigid molecule, its R_h is independent of refractive index and viscosity. R_h of C480 was determined using eq 6 from the known value of D_t of C480 in bulk water (600 $\mu m^2/s$).[21b] We determined the diffusion time of free C480 in different solutions of GdnHCl and RTIL concentration without the protein sample for each experiment. The standardization with free C480 probe mimics the exact experimental condition to minimize the effect due to viscosity and the refractive index.

3. RESULTS AND DISCUSSION

3.1. FRET from Tryptophan to Labeled CPM in HSA: Steady State Experiment. As mentioned earlier, HSA has a single tryptophan residue (in domain IIa).[17] The distance between the lone tryptophan to CPM labeled to the cys-34 residue of HSA is determined by steady state FRET experiment (Figure 1). The tryptophan emission for the CPM labeled HSA is quenched compared to that of the same concentration of the HSA without CPM, due to the presence of acceptor CPM in the HSA molecule. We have determined the degree of labeling by the method of incorporation calculation, and it is found to be 1:1. So the extent of labeling does not affect the efficiency of energy transfer in our experiment. The FRET efficiency (E_{FRET}) is calculated from the following equation:

$$E_{FRET} = 1 - \frac{I}{I_0} \tag{8}$$

where I is the fluorescence intensity of the tryptophan (donor) in the presence of CPM (acceptor) covalently bound to HSA and I_0 is the fluorescence intensity of the tryptophan in the absence of any CPM. The FRET efficiency (E_{FRET}) from tryptophan to CPM is calculated to be 30%. The FRET efficiency (E_{FRET}) is related to the donor−acceptor distance (r)

$$E_{FRET} = \frac{{R_0}^6}{r^6 + {R_0}^6} \tag{9}$$

where R_0 is the Förster distance (the distance at which energy transfer is 50% efficient). The Förster distance (R_0) for energy transfer from tryptophan to CPM (at λ_{ex} = 280 nm) is calculated to be 26 Å with overlap integral $J(\lambda) = 2.6 \times 10^{14}$ M^{-1} cm^{-1} nm^4. Finally, the exact distance (r) from tryptophan to CPM is calculated to be 30 Å by using eq 9.

3.2. Circular Dichroism (CD) Spectra. Figure 2A describes the effect of GdnHCl on the circular dichroism (CD) spectra of HSA and, in particular, the alpha helical structure of the protein. The CD spectrum of HSA exhibits two minima at 208 nm and another at 222 nm, representing the alpha helical structure of the protein. On addition of GdnHCl, the differential absorption intensity (CD) for both the minima decreases. This is a clear indication of unfolding or uncoiling of HSA. As shown in Figure 2A, in 1 M GdnHCl, the protein retains 97% of its helical structure while the amount of helical structure reduces to 53% and 34% in the presence of 3 and 6 M GdnHCl, respectively.

Table 3. Effect of a RTIL on the Diffusion (ms) and Relaxation (μs) Time of Denatured (with 6 M GdnHCl) Human Serum Albumin (HSA) Labeled with CPM

[pmim][Br]	τ_D (ms)	τ_{R1} (μs) (A_1)	τ_{R2}(μs) (A_2)	τ_{R3} (μs) (A_3)	D_t ($\mu m^2/s$)	R_h (Å)
0 M	0.765 ± 0.04	3.2 ± 0.4 (0.16)	34 ± 6 (0.43)	207 ± 38 (0.41)	29.4 ± 1.5	61.0 ± 3.0
0.3M	0.87 ± 0.04	6.0 ± 1.1 (0.30)	40 ± 9 (0.39)	265 ± 50 (0.31)	25.9 ± 1	59.4 ± 2.7
0.9 M	0.84 ± 0.04	6.1 ± 0.8 (0.23)	42 ± 7 (0.42)	245 ± 42 (0.35)	26.8 ± 1.2	48.9 ± 2.0
1.5 M	0.82 ± 0.03	5.0 ± 1 (0.22)	41 ± 10 (0.40)	230 ± 45 (0.38)	27.4 ± 1	41.2 ± 1.5

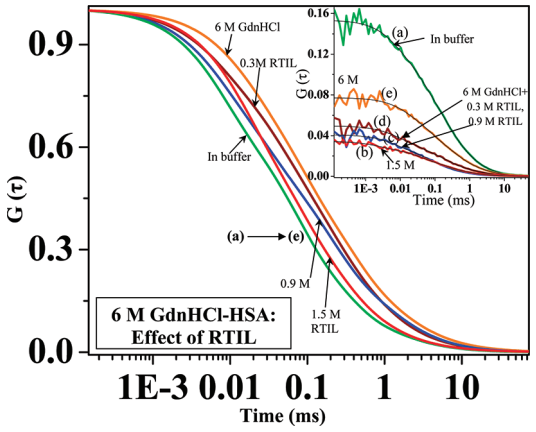

Figure 6. The normalized fit lines of the autocorrelation curves of CPM labeled HSA in the presence of (a) buffer and (e) 6 M GdnHCl, i.e., under fully denatured conditions. However, the autocorrelation traces become faster with gradual addition of RTIL, (b) 1.5 M [pmim][Br], (c) 0.9 M [pmim][Br], and (d) 0.3 M [pmim][Br], under fully denatured conditions. The inset shows the original autocorrelation curves with their best fit line.

Because of the large absorbance of the RTIL in the far UV range (200−235 nm), the CD background of [pmim][Br] is too noisy to reveal the effect of the RTIL on the secondary structure of the HSA. Thus, to understand the effect of RTIL on the conformation of the native protein, differential absorption was studied in the range 235−500 nm.

Figure 2B describe the effect of RTIL on the structure of the HSA in the absence and presence of GdnHCl. The decrease in CD signal in the range 235−250 nm suggests uncoiling of the protein on addition of RTIL. This is consistent with previous CD studies on RTIL induced change of structure of a protein.[13]

In the presence of GdnHCl, there is considerable difference in the CD spectrum (Figure 2C) of the protein in the presence and absence of RTIL. This suggests that the structure of the protein denatured by GdnHCl is substantially different on addition of RTIL. In summary, addition of RTIL considerably modifies the structure of the HSA in the presence or absence of GdnHCl.

3.3. Fluctuation of Fluorescence Intensity and FCS Trace of CPM Labeled HSA. The main sources of fluctuation are diffusion of the labeled protein in and out of the focus. From this, the size of the protein may be determined using the Stokes−Einstein equation (eq 6). The second source of fluctuation is quenching of the fluorescence by the amino groups of the protein. This happens because of the conformational dynamics of the protein when an amino group comes in close vicinity of the fluorophore (CPM). Thus, the FCS traces yield information on both the size (diffusion coefficient) and conformational dynamics of the protein.

3.3.1. FCS Trace of Native HSA: Effect of RTIL. Figure 3 shows FCS autocorrelation of CPM covalently attached to HSA in phosphate buffer at different RTIL concentrations. The figure clearly demonstrates that there is an increase of the number of particles (N) in the focal volume with the increase of the concentration of RTIL. This is due to refractive index mismatch. Addition of RTIL (η = 110 cP) to covalently labeled HSA solution causes a drastic change in viscosity. We have corrected both the errors in our data, as described earlier in the Experimental Section (2.3).

The autocorrelation traces were fitted to a 3-component-3D diffusion model (eq 5) to obtain the diffusion time (τ_D). From the value of τ_D, the diffusion coefficient (D_t) was calculated, and subsequently, from τ_D, the hydrodynamic radius (R_h) is determined using eq 7.

Table 1 lists D_t and R_h of CPM labeled HSA in the presence of different RTIL concentrations. With gradual addition of RTIL, the diffusion time (τ_D) of the protein gradually increases from 0.4 ± 0.02 ms (400 ± 20 μs) in 0 M RTIL to 1.2 ± 0.04 ms (1200 ± 40 μs) in the presence of 1.5 M RTIL. This corresponds to an increase in the hydrodynamic radius of the HSA from 38.4 ± 2 Å (in 0 M RTIL) to 60.9 ± 2 Å (in 1.5 M RTIL). Thus, addition of RTIL causes an ∼3-fold increase of diffusion time and ∼60% increase in the hydrodynamic radius (R_h) of the HSA. The increase in the hydrodynamic radius of HSA implies that RTIL acts as a denaturant when added to native HSA protein. This is consistent with previously reported results of denaturation of protein by RTIL.[10−13]

By fitting of the FCS traces to a 3-component-3D diffusion model, we obtained, apart from diffusion time (τ_D), three relaxation time components (τ_R) which arise from the conformational dynamics of the protein. In the native state of the protein (HSA), the three components are ∼3.6 ± 0.7, ∼29 ± 4.5, and 133 ± 23 μs. Following the early analysis of the Webb group on another protein,[1b] we assign the two faster components (∼3.6 ± 0.7 and ∼29 ± 4.5 μs) to chain dynamics. The slowest component (133 ± 23 μs) is attributed to the concerted chain motion or interchain interaction. With gradual addition of RTIL, the time components gradually increase. At 1.5 M RTIL, the time components become ∼5.1 ± 1, ∼43.5 ± 8, and 311 ± 50 μs. The slower relaxation in the presence of the RTIL may arise from higher local viscosity and interaction of the ions of the RTIL with polar residues of the protein. It may be mentioned that the slowest components of the conformational relaxation (133 ± 23 μs in 0 M RTIL and 311 ± 50 μs in 1.5 M RTIL) are much faster than the diffusion time of the protein (400 ± 20 μs in 0 M RTIL and 1200 ± 40 μs in 1.5 M RTIL).

3.3.2. FCS Trace of HSA: Effect of GdnHCl. Several groups showed that GdnHCl acts as a denaturant and plays an important role in unfolding of HSA. In the absence of GdnHCl, HSA shows a diffusion time (τ_D) of 0.4 ± 0.02 ms in phosphate buffer which corresponds to a hydrodynamic radius (R_h) of 38.4 ± 2 Å.

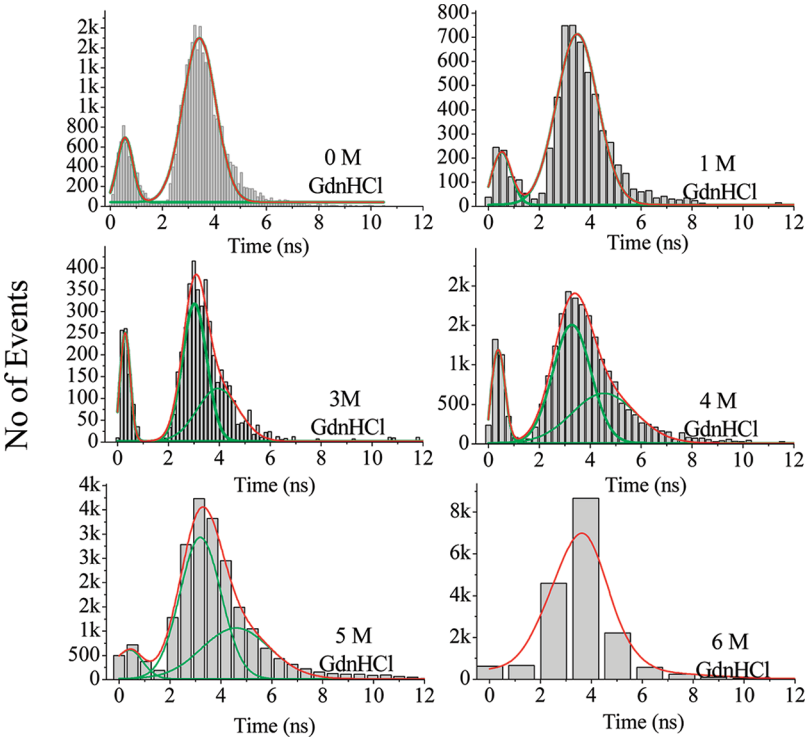

Figure 7. Lifetime histogram of CPM bounded to the human serum albumin (HSA) in the native state and at different concentrations of denaturant (GdnHCl). The solid red lines are the overall fit line, and the green lines are the histogram fit line for the individual lifetime component.

The reported radius of HSA in the absence of denaturant is 36 ± 1 Å using SAXS.[22] Thus, our calculated hydrodynamic radius of HSA (R_h) using FCS is in good agreement with the reported value.

From Figure 4 and Table 2, it is apparent that, with gradual addition of GdnHCl, τ_D and the corresponding hydrodynamic radius (R_h) of the protein gradually increase. Initially, up to 2 M GdnHCl, the diffusion time and hydrodynamic radius do not increase appreciably (from τ_D = 0.4 ± 0.02 ms, R_h = 38.4 ± 2 Å at 0 M GdnHCl to 0.48 ± 0.03 ms, 43.1 ± 2.5 Å at 2 M GdnHCl). This is very consistent with the SAXS data.[22]

However, there is a rapid increase of τ_D and hydrodynamic radius for [GdnHCl] > 2 M (e.g., at ∼4 M GdnHCl, τ_D = 0.66 ± 0.03 ms, R_h = 56.6 ± 2.5 Å). At 6 M GdnHCl, the diffusion time (τ_D) becomes 0.77 ± 0.04 ms and R_h is 61 ± 3 Å (Figure 5). Thus, during denaturation by GdnHCl, the hydrodynamic radius of HSA increases by ∼60%. This result is also in good agreement with the previous studies[22] and with the CD spectra. For the determination of R_h of highly denatured protein from NMR, Willkins et al.[23] proposed an empirical formula

$$R_h = (2.11 \pm 0.15)N^{0.57 \pm 0.02} \quad (10)$$

where N is the number of amino acid residues in the protein. Using this relation, we calculated the R_h of HSA to be 70 ± 5 Å for 585 amino acid residues. This result is also very close to our calculated hydrodynamic radius (61 ± 3 Å) of the denatured HSA using FCS.

With gradual addition of GdnHCl, the chain dynamics and concerted chain motion become slower. In 1 M GdnHCl, the relaxation components are, respectively, 3.5 ± 0.5, 22 ± 5, and 124 ± 20 μs. At 6 M GdnHCl, the time constants for chain dynamics and concerted chain motion become ∼3.2 ± 0.4, ∼34 ± 6, and 207 ± 38 μs, respectively. In fully unfolded conditions, the relaxation component for concerted motion increases by 66%.

3.3.3. FCS Trace of HSA Unfolded by 6 M GdnHCl: Effect of RTIL. Addition of RTIL to HSA denatured by 6 M GdnHCl causes ∼90% recovery of the hydrodynamic radius (folded state) (Figure 6, Table 3). The hydrodynamic radius of the denatured HSA in the presence of 0.3 M RTIL is 59.4 ± 2.7 Å, which decreases to 41 ± 1.5 Å in the presence of 1.5 M RTIL. This is close to the hydrodynamic radius of the native protein (38.4 ± 2 Å). This result clearly demonstrates that the RTIL acts as a stabilizer of a protein if it is added in the unfolded states. This is consistent to the previously reported results that RTIL acts as a stabilizer of the unfolded protein.[15]

The diffusion time (τ_D) of the unfolded state of HSA in the presence of 0.3 M RTIL is 0.87 ± 0.04 ms, and the time components (τ_R) of conformational relaxation are 6 ± 1, 40 ± 9, and 265 ± 50 μs. In the presence of 1.5 M RTIL, the diffusion time (τ_D) decreases to 0.82 ± 0.03 ms and the time components (τ_R) of conformation dynamics decrease to 5 ± 1, 41 ± 10, and 230 ± 45 μs.

3.4. Burst Integrated Florescence Lifetime (BIFL) Histogram of CPM Covalently Bound to HSA: Effect of RTIL. The burst integrated fluorescent lifetime (BIFL)[24,25] histogram of CPM covalently labeled to HSA displays a distribution of lifetimes with two maxima (Figure 7). The shorter lifetime (∼450 ps) is attributed to an exposed location of HSA molecule. The longer lifetime of ∼4000 ps is attributed to a buried location of the HSA molecule. On addition of the denaturant (GdnHCl), the amplitude of the shorter lifetime component decreases. Most interestingly, the shorter lifetime component vanishes in the presence of the 6 M concentration of GdnHCl. This may suggest that the denatured protein contains some small hydrophobic and buried pockets in which the fluorescence probe (CPM) remains

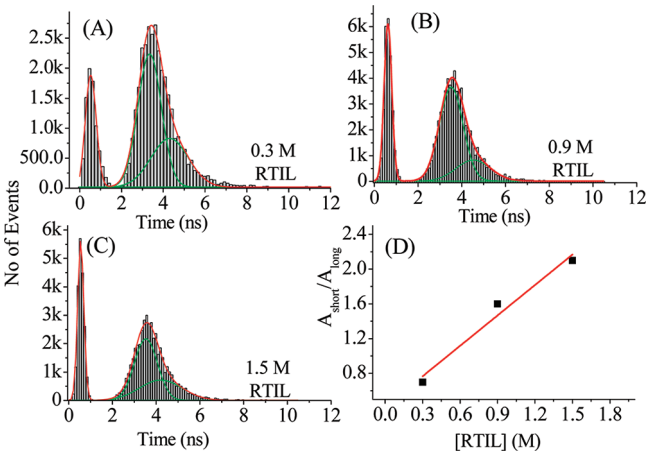

Figure 8. Lifetime histogram of CPM bounded to the human serum albumin (HSA) at different concentrations of RTIL: (A) 0.3 M, (B) 0.9 M, and (C) 1.5 M. The solid red lines are the overall fit line, and the green lines are the histogram fit line for the individual lifetime component. (D) The ratio of amplitude of the short and long time component (A_{short}/A_{long}) is plotted against concentration (M) of added RTIL.

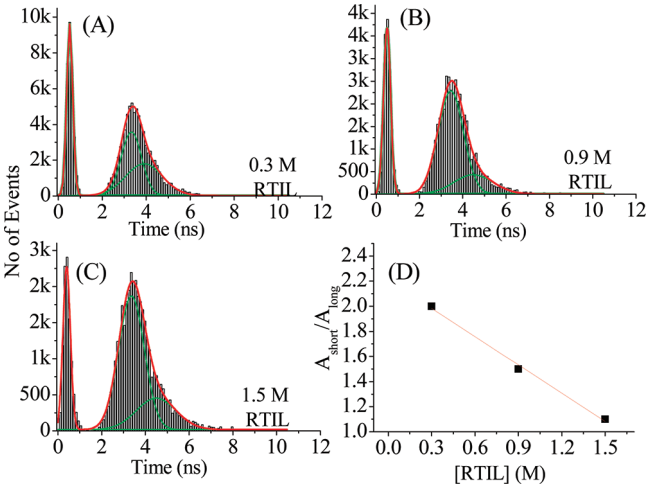

Figure 9. Lifetime histogram of CPM bounded to the human serum albumin (HSA) at different concentrations of RTIL in the presence of 6 M GdnHCl (fully denatured conditions). The solid red lines are the overall fit line, and the green lines are the histogram fit line for the individual lifetime component.

bound. It may be noted that such small pockets in a denatured protein have been proposed earlier.[6c]

Figure 8 shows the lifetime histogram of the CPM molecule bound to the HSA in addition to the different concentrations of the RTIL. On addition of RTIL to the native HSA, the contribution of the shorter component (exposed site) increases (Figure 8D).

Figure 9 shows the lifetime histogram of the CPM bound to unfolded HSA (by GdnHCl) with increasing concentration of the RTIL. Most interestingly, the 450 ps component immediately appears with the addition of the RTIL with unfolded HSA. This once again indicates RTIL induced refolding of denatured HSA. Again, with the increase of RTIL, the amplitude of the slowest component increases. Figure 10 shows the lifetime

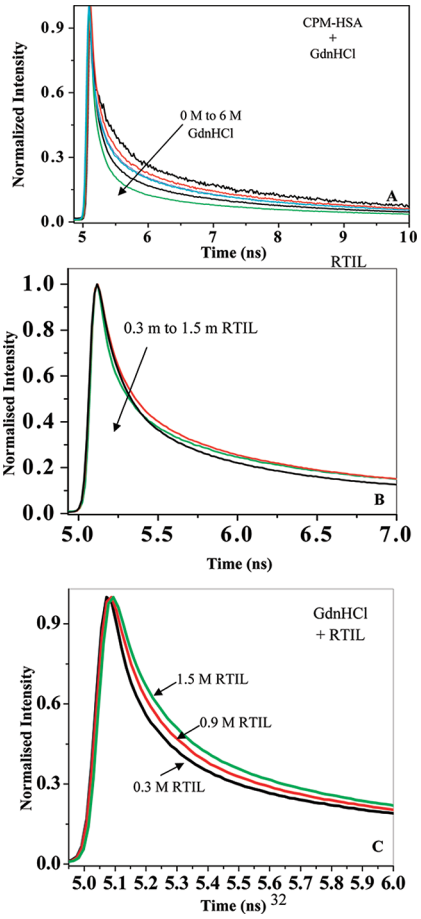

Figure 10. Lifetime decay of CPM labeled with HSA in the presence of (A) GdnHCl, (B) only RTIL, and (C) RTIL under fully denatured conditions (with 6 M GdnHCl).

decays of CPM labeled HSA at different GdnHcl and RTIL concentrations. The lifetime decays well support the results obtained from the BIFL studies.

4. CONCLUSION

This work demonstrates that FCS may be used to study the effect of RTIL on the size (diffusion) and conformational dynamics of a protein HSA in the native and the unfolded (by GdnHCl) state. It was shown that addition of RTIL increases size and slows down dynamics of the protein in the native state. However, for the unfolded protein addition of RTIL causes a decrease in size and makes the dynamics faster. It is proposed that RTIL unfolds the protein in the native state and refolds the unfolded state. The time constants (τ_R) for conformational dynamics of the protein during unfolding and refolding were also determined. The two faster time components (3−40 μs) are ascribed to chain dynamics of the protein, while the slowest component (100−300 μs) is responsible for interchain interaction or concerted motion. From steady-state FRET, the distance from the single tryptophan to the CPM at cys-34 is found to be ∼30 Å. Denaturation of HSA by GdnHCl causes the increase of the hydrodynamic radius of HSA by ∼60%. Similarly, addition of RTIL causes an ∼3-fold increase of diffusion time (D_t) and ∼60% increase in the hydrodynamic radius (R_h) of the HSA. Addition of RTIL to denatured HSA causes ∼90% recovery of

the folded state. The lifetime histogram shows that the amplitude of the shorter lifetime component gradually decreases with the increase of concentration of GdnHCl, and it vanishes in 6 M GdnHCl. This shorter lifetime component immediately reappears after the addition of the RTIL in the unfolded state of HSA which is a clear indication of the refolding of the denatured HSA.

AUTHOR INFORMATION

Corresponding Author

*E-mail: pckb@iacs.res.in. Fax: (91)-33-2473-2805.

ACKNOWLEDGMENT

Thanks are due to Department of Science and Technology, India (Centre for Ultrafast Spectroscopy and Microscopy Project and J. C. Bose Fellowship) and the Council of Scientific and Industrial Research (CSIR) for generous research support. D.K.S., T.M., and S.S.M. thank CSIR for awarding fellowships.

REFERENCES

(1) (a) Elson, E. L.; Magde, D. *Biopolymers* **1974**, *13*, 1–27. (b) Chen, H.; Rhoades, E.; Butler, J. S.; Loh, S. N.; Webb, W. W. *Proc. Natl. Acad. Sci. U.S.A.* **2007**, *104*, 10459–10464. (c) Haupts, U.; Maiti, S.; Schwille, P.; Webb, W. W. *Proc. Natl. Acad. Sci. U.S.A.* **1998**, *95*, 13573–13578.

(2) (a) Tan, X.; Hu, D.; Tan, X.; Lu., H. P. *J. Am. Chem. Soc.* **2006**, *128*, 10034–10042. (b) Liu, R.; Nalbant, P.; Toutchkine, A.; Hu, D.; Vorpagel, E. R.; Hahn, K. M.; Lu., H. P. *J. Phys. Chem. B* **2004**, *108*, 737–744.

(3) Kim, H. D.; Nienhaus, G. U.; Ha, T.; Orr, J. W.; Williamson, J. R.; Chu, S. *Proc. Natl. Acad. Sci. U.S.A.* **2002**, *99*, 4284–4289.

(4) (a) Kim, J.; Doose, S.; Neuweiler, H.; Sauer, M. *Nucleic Acids Res.* **2006**, *34*, 2516–2527. (b) Neuweiler, H.; Johnson, C. M.; Fersht, A. R. *Proc. Natl. Acad. Sci. U.S.A.* **2009**, *106*, 18569–18574.

(5) Li, H. T.; Ren, X. J.; Ying, L. M.; Balasubramanium, S.; Klenerman, D. *Proc. Natl. Acad. Sci. U.S.A.* **2004**, *101*, 14425–14430.

(6) (a) Chattopadhyay, K.; Saffarian, S.; Elson, E. L.; Frieden, C. *Proc. Natl. Acad. Sci. U.S.A.* **2002**, *99*, 14171–14176. (b) Chattopadhyay, K.; Saffarian, S.; Elson, E. L.; Frieden, C. *Biophys. J.* **2005**, *88*, 1413–1422. (c) Ghosh, R.; Sharma, S.; Chattopadhyay, K. *Biochemistry* **2009**, *48*, 1135–1143.

(7) Sherman, E.; Itkin, A.; Kuttner, Y. Y.; Rhoades, E.; Amir, D.; Haas, E.; Haran, G. *Biophys. J.* **2008**, *94*, 4819–4827.

(8) (a) Horvath, I. T.; Anastas, P. T. *Chem. Rev.* **2007**, *107*, 2169–2173. (b) van Rantwijk, F.; Sheldon, R. A. *Chem. Rev.* **2007**, *107*, 2757–2785.

(9) (a) Wei, D.; Ivaska, A. *Anal. Chim. Acta* **2008**, *607*, 126–135. (b) Weuster-Botz, D. *Chem. Rec.* **2007**, *7*, 334–340.

(10) (a) Byrne, N.; Wang, L. M.; Belieres, J. P.; Angell, C. A. *Chem. Commun.* **2007**, 2714–2716. (b) Constatinescu, D.; Herrmann, C.; Weingartner, H. *Phys. Chem. Chem. Phys.* **2010**, *12*, 1756–1763. (c) Mann, J. P.; McCluskey, A.; Atkin, R. *Green Chem.* **2009**, *11*, 785–792.

(11) Fujita, K.; MacFarlane, D. R.; Forsyth, M.; Yoshizawa-Fujita, M.; Murata, K.; Nakamura, N.; Ohno, H. *Biomacromolecules* **2007**, *8* (7), 2080–2086.

(12) Baker, S. N.; McCleskey, T. M.; Pandey, S.; Baker, G. A. *Chem. Commun.* **2004**, 940–941.

(13) (a) Heller, W. T.; O'Neill, H. M.; Zhang, Q.; Baker, G. A. *J. Phys. Chem. B* **2010**, *114*, 13866–13871. (b) Bihari, M.; Russell, T. P.; Hoagland, D. A. *Biomacromolecules* **2010**, *11*, 2944–2948. (c) Mann, J. P.; McCluskey, A.; Atkin, R. *Green Chem.* **2009**, *11*, 785–792. (d) Wei, W.; Danielson, N. D. *Biomacromolecules* **2011**, *12*, 290–297. (e) Page, T. A.; Kraut, N. D.; Page, P. M.; Baker, G. A.; Bright, F. V. *J. Phys. Chem. B* **2009**, *113*, 12825–12830. (f) Akdogan, Y.; Junk, M. J. N.; Hinderberger, D. *Biomacromolecules* **2011**, *12*, 1072–1079. (g) McCarty, T. A.; Page, P. M.; Baker, G. A.; Bright, F. V. *Ind. Eng. Chem. Res.* **2008**, *47*, 560–569.

(14) Micaêlo, N. M.; Soares, C. M. *J. Phys. Chem. B* **2008**, *112*, 2566–2572.

(15) (a) Summers, C. A.; Flowers, R. A., II. *Protein Sci.* **2000**, *9*, 2001–2008. (b) Lange, C.; Patil, G.; Rudolph, R. *Protein Sci.* **2005**, *14*, 2693–2701.

(16) (a) Curry, S.; Mandelcow, H.; Brick, P.; Franks, N. *Nat. Struct. Biol.* **1998**, *5*, 827–835. (b) Curry, S.; Brick, P.; Franks, N. P. *Biochim. Biophys. Acta, Mol. Cell Biol. Lipids* **1999**, *1441*, 131–140. (c) Bhattacharya, A. A.; Gruine, T.; Curry, S. *J. Mol. Biol.* **2000**, *303*, 721–732.

(17) (a) Sudlow, G.; Birkett, D. J.; Wade, D. N. *Mol. Pharmacol.* **1976**, *12*, 1052. (b) Sudlow, G.; Birkett, D. J.; Wade, D. N. *Mol. Pharmacol.* **1976**, *11*, 824–832. (c) Das, D. K.; Mondal, T.; Mandal, A. K.; Bhattacharyya, K. *Chem. Asian J.* **2011**, DOI: 10.1002/asia.201100272.

(18) Mandal, U; Ghosh, S.; Mitra, G.; Adhikari, A.; Dey, S.; Bhattacharyya, K. *Chem. Asian J.* **2008**, *3*, 1430–1434.

(19) (a) Wang, R.; Sun, S.; Bekos, E.; Bright, F. V. *Anal. Chem.* **1995**, *67*, 149–159. (b) Lowry, O. H.; Rosebrough, N. J.; Farr, A. L.; Randall, R. J. *J. Biol. Chem.* **1951**, *193*, 265–275.

(20) (a) Sasmal, D. K.; Mondal, T.; Bhattacharyya, K. *J. Phys. Chem. B* **2011**, *115*, 7781–7787. (b) Sasmal, D. K.; Sen Mojumdar, S.; Adhikari, A.; Bhattacharyya, K. *J. Phys. Chem. B* **2010**, *114*, 4565–4571.

(21) (a) Petrasek, Z.; Schwille, P. *Biophys. J.* **2008**, *94*, 1437–1448. (b) Ghosh, S.; Mandal, U.; Adhikari, A.; Bhattacharyya, K. *Chem. Asian J.* **2009**, *4*, 948–954.

(22) Galantini, L.; Leggio, C.; Konarev, P. V.; Pavel, N. V. *Biophys. Chem.* **2010**, *147*, 111–122.

(23) Wilkins, D. K.; Grimshaw, S. B.; Receveur, V.; Dobson, C. M.; Jones, J. A.; Smith, L. J. *Biochemistry* **1999**, *38*, 16424–16431.

(24) Eigen, M.; Rigler, R. *Proc. Natl. Acad. Sci. U.S.A.* **1994**, *91*, 5740–5747.

(25) (a) Eggeling, C.; Fries, J. R.; Brand, L.; Gunther, R.; Seidel, C. A. M. *Proc. Natl. Acad. Sci. U.S.A.* **1998**, *95*, 1556–1561. (b) Al-Soufi, W.; Reija, B.; Felekyan, S.; Seidel, C. A. M.; Novo, M. *ChemPhysChem* **2008**, *9*, 1819–1827.